

Num erical study of discrete m odels in the class of the nonlinear m olecular beam epitaxy equation

F . D . A . A arao Reis

Instituto de F ísica, Universidade Federal Fluminense,
Avenida Litorânea s/n, 24210-340 N iterói RJ, Brazil
(March 22, 2024)

We study num erically some discrete growth m odels belonging to the class of the nonlinear m olecular beam epitaxy equation, or Villain-Lai-D as Sarm a (V L D S) equation. The conserved restricted solid-on-solid m odel (CRSOS) with m axim um heights differences $H_{m ax} = 1$ and $H_{m ax} = 2$ was analyzed in substrate dimensions $d = 1$ and $d = 2$. The D as Sarm a and Tam borenea (D T) m odel and a com petitive m odel involving random deposition and CRSOS deposition were studied in $d = 1$. For the CRSOS m odel with $H_{m ax} = 1$ we obtain the m ore accurate estim ates of scaling exponents in $d = 1$: roughness exponent $\alpha = 0.94 \pm 0.02$ and dynam ical exponent $z = 2.88 \pm 0.04$. These estim ates are signi cantly below the values of one-loop renorm alization for the V L D S theory, which con firm s Janssen's proposal of the existence of higher order corrections. The roughness exponent in $d = 2$ is very near the one-loop result $\alpha = 2/3$, in agreement with previous works. The m om ents W_n of orders $n = 2, 3, 4$ of the heights distribution were calculated for all m odels and the skewness $S = W_3/W_2^{3/2}$ and the kurtosis $Q = W_4/W_2^2 - 3$ were estim ated. At the steady states, the CRSOS m odels and the com petitive m odel have nearly the sam e values of S and Q in $d = 1$, which suggests that these am plitude ratios are universal in the V L D S class. The estim ates for the D T m odel are different, possibly due to their typically long crossover to asym ptotic values. Results for the CRSOS m odels in $d = 2$ also suggest that those quantities are universal.

PACS numbers: 05.40.-a, 05.50.+q, 81.15.Aa

Keywords: deposition m odels; thin films; m olecular beam epitaxy; interface growth; universality classes; scaling exponents.

I. INTRODUCTION

Surface and interface growth processes are subjects of great interest for the perspective of applications to thin films and multilayers growth and, from the theoretical point of view, for their im portant role in Non-E quilibrium Statistical M echanics [1,2]. Frequently those processes are described by discrete m odels which represent the basic growth m echanism s by simple stochastic rules, such as aggregation and di usion, and neglect details of the m icroscopic interactions. On the other hand, continuous theories are successful at representing those processes in the hydrodynam ic limit. They predict the scaling exponents of m any discrete m odels, which are consequently grouped in a sm all num ber of universality classes.

G rowth by m olecular beam epitaxy (M B E), which is one of the m ost im portant techniques to produce high quality films with sm ooth surfaces, motivated the proposal of m any discrete and continuous m odels. The dynam ics during M B E deposition is dom inated by di usion processes, which led to the proposal of an im portant theoretical m odel, the Villain-Lai-D as Sarm a (V L D S) growth equation [3,4]

$$\frac{\partial h}{\partial t} = \kappa_4 r^4 h + \kappa_4 r^2 (r h)^2 + \xi(\mathbf{x}; t); \quad (1)$$

where $h(\mathbf{x}; t)$ is the height at position \mathbf{x} and time t in a d -dim ensional substrate, κ_4 and κ_4 are constants and ξ is a Gaussian (nonconservative) noise. Eq. (1) is also

frequently called nonlinear m olecular beam epitaxy equation or conserved Kardar-Parisi-Zhang equation [1,5],

The m ost im portant geom etrical quantity to characterize the surface of the deposit grown by such processes is the interface width. It is defined as the root m ean square fluctuation of the average height

$$h_D = \sqrt{\frac{1}{h} \sum_i h_i^2} : \quad (2)$$

For short times, it scales as

$$h_D \sim t^\alpha; \quad (3)$$

where α is called the growth exponent. For long times, in the steady state, the interface width saturates at

$$h_{sat} \sim L^{-\alpha}; \quad (4)$$

where α is called the roughness exponent. The crossover time from the growth regime to the steady state scales with L with the dynam ical exponent

$$z = \alpha + \alpha : \quad (5)$$

For the V L D S theory, a one-loop dynam ical renorm alization-group (D R G) calculation [3,4] led to $\alpha = (4 - d)/3$, $z = (8 + d)/3$ and $\alpha = (4 - d)/(8 + d)$ below the upper critical dimension $d_c = 4$. See also the recent work of Katzav [6], based on a self-consistent expansion approach, which also obtains these estim ates. Some authors assumed the one-loop values to be exact in all orders, but Janssen [7] recently claimed that this conclusion

was derived from an ill-defined transformation and, consequently, there would be higher order corrections. From a two-loop calculation, he obtained small negative corrections to α and z in all dimensions [7]. Numerical studies of some discrete models which belong to the VLD S class in the continuum limit (large lattices, long times) were not able to solve this controversy. In $d = 1$, numerical work on a conserved restricted solid-on-solid model (to be defined below) systematically suggests $\alpha < 1$ [8,9], but the error bars are large and, consequently, the authors still suggest the validity of the one-loop result. In $d = 2$ and higher dimensions [10], numerical results indicated that possible corrections to the one-loop result were smaller than the two-loops estimates of Janssen [7].

Another important question is motivated by recent results on discrete models belonging to the Kardar-Parisi-Zhang (KPZ) class in $d = 2$. The KPZ growth equation includes second order linear and nonlinear terms which are more relevant than those in the VLD S equation (Eq. 1) in the hydrodynamic limit [5,1]. Works on discrete KPZ models showed that the steady state values of the moments of the height distribution,

$$W_n = \frac{D}{h} \frac{E}{h^n}; \quad (6)$$

obey power-counting, i. e. they scale as

$$W_n \sim L^n \quad (7)$$

(note that $W_2 = \alpha^2$). Moreover, estimates of the skewness

$$S = \frac{W_3}{W_2^{3/2}} \quad (8)$$

and of the kurtosis

$$Q = \frac{W_4}{W_2^2} - 3 \quad (9)$$

of the KPZ models indicated that the amplitude ratios of the moments W_n (such as S and Q) are universal [11,13]. It seems that no previous work has considered these questions in models belonging to the VLD S class, possibly due to the large times involved in their simulations (the dynamical exponent is nearly the double of the KPZ value). Besides the theoretical relevance of those questions, additional motivation for their analysis is the fact that the amplitude ratios can be measured with much higher accuracy than the scaling exponents and may eventually help one to infer the universality class of an experimental growth process.

There is a small number of discrete models belonging to the VLD S class in the continuum limit. The discrete model proposed by Das Sarma and Tamborenea (DT model) [14] is an example of a MBE-motivated model which falls in that class in $d = 1$, although there is evidence that its class in $d = 2$ is different [15,16]. On the other hand, the so-called conserved restricted-solid-on-solid (CRSOS) models, first proposed by Kim et al [8], is

expected to belong to the VLD S class in all dimensions. This was already proved analytically in $d = 1$ [17,19]. In the CRSOS models, the difference of the heights of neighboring columns are always smaller than a certain value

H_{max} , similarly to the RSOS model of Kim and Kosterlitz [20,21]. However, in the Kim-Kosterlitz model, if the aggregation at the column of incidence does not satisfy that condition, then the aggregation attempt is rejected (consequently, the model is in the KPZ class). On the other hand, in the CRSOS model, the incident particle migrates to the nearest column at which the height difference constraint is satisfied after aggregation. Thus, all deposition attempts are successful in the CRSOS model.

Here, we will study numerically a modified version of the CRSOS model in $d = 1$ and $d = 2$, with two different values of H_{max} , the DT model in $d = 1$, simulated with noise-reduction methods, and a competitive model involving CRSOS and random deposition in $d = 1$. All these models belong to the VLD S class. We will perform systematic extrapolations of effective (roughness and dynamical) exponents for the CRSOS model in $d = 1$ and $d = 2$. The asymptotic exponents in $d = 1$ are clearly different from the one-loop DRG values and the sign of the deviations are in qualitative agreement with Janssen's results [7]. In $d = 2$, possible corrections in the exponent are smaller than the two-loop corrections calculated in that work, confirming other authors' conclusions. It will also be shown that the moments of the heights distribution obey power-counting (Eq. 7) in $d = 1$ and $d = 2$, similarly to KPZ, and that the skewness and the kurtosis for different versions of the CRSOS model (different H_{max}) and for the competitive model have nearly the same values. These estimates differ from those of the DT model in $d = 1$, but universality of amplitude ratios in the VLD S class cannot be discarded due to the typical long crossovers of the DT model.

The rest of this paper is organized as follows. In Sec. II we present the stochastic rules of the CRSOS and DT models and give information on the simulation procedure. In Sec. III, we calculate the scaling exponents of the VLD S class in one-dimensional substrates. In Sec. IV, we calculate the scaling exponents in two-dimensional substrates. In Sec. V, we compare the asymptotic amplitude ratios of all models in $d = 1$ and $d = 2$. In Sec. VI we summarize our results and present our conclusions.

II. MODELS AND SIMULATION PROCEDURE

The rules for choosing the aggregation point in our version of the CRSOS model are slightly different from the original ones. The present version was introduced in Ref. [22] as a model for amorphous carbon-nitrogen film growth, but only small lattices were analyzed there and, consequently, reliable estimates of scaling exponents were not obtained.

At any time, all pairs of neighboring columns are re-

stricted to obey the condition $h_i \leq H_{\max}$, where h_i is the difference in the columns' heights and H_{\max} is fixed. The deposition attempt begins with the random choice of one substrate column i . If the above condition is satisfied after aggregation of a new particle at the top of column i , then the aggregation takes place at that position. Otherwise, a nearest neighbor column is randomly chosen (independently of its height) and the same test is performed. This process is continued until a column is chosen in which the new particle can be permanently deposited. Here, the cases $H_{\max} = 1$ and $H_{\max} = 2$ will be analyzed.

In the original version of the CRSOS model [8], the aggregation takes place at the nearest column in which the condition on heights differences is satisfied, but in our version the incident particle performs a random walk along the substrate direction (s) while it searches for the aggregation point. The original model was proved to belong to the VLD class in $d = 1$ by different methods [17,19] and the coefficients of the VLD equation were explicitly calculated for $H_{\max} = 1$ [18,19]. Since our version does not change any symmetry of the original CRSOS model, it is also expected to be in that class. Notice, for instance, that there is no upward or downward current in our model due to the mechanism of random walks for choosing the aggregation position (the random steps do not depend on the relative heights of the columns). It implies that the coefficient of the second order height derivative of the growth equation (not shown in Eq. 1) is exactly zero, the VLD equation being the most plausible continuum description – see e. g. the discussion in Ref. [23].

We will also study the DT model in $d = 1$. In this model, the incident particle sticks at the top of the randomly chosen column i if it has one or two lateral neighbors at that position (a kink site or a valley, respectively). Otherwise, the neighboring columns (at the right and the left sides in $d = 1$) are consulted. If the top position of only one of these columns is a kink site or a valley, then the incident particle aggregates at that point. If no neighboring column satisfies that condition, then the particle sticks at the top of column i . Finally, if both neighboring columns satisfy that condition, then one of them is randomly chosen.

In our simulations of the DT model, we used the noise reduction technique adopted in Ref. [24]. The noise reduction factor m is the number of attempts at a site for an actual aggregation process to occur [25,26]. Here, the value $m = 10$ will be considered because it provided accurate estimates of scaling exponents in Ref. [24] from simulations in relatively small systems. On the other hand, the data for the original DT model present huge finite-size corrections (see e. g. Ref. [27]).

In order to improve our discussion on the universality of amplitude ratios (Sec. V), we also simulated a competitive model in which the aggregation of the incident particle may follow two different rules: with probability p , the particle aggregates at the top of the column of incidence,

such as in the random deposition (RD) model [1]; otherwise (probability $1 - p$), it diffuses until finding a column i in which the condition $h_i \leq h_j \leq H_{\max}$ is satisfied for all nearest neighbors j after aggregation. Thus, the latter aggregation mechanism works for preserving the columns heights' constraint of the CRSOS model. Extending previous conclusions on other competitive models [28,29], it is expected that this model is described asymptotically by the VLD equation, similarly to the pure CRSOS model, but the coefficients α_4 and α_6 of the corresponding continuous equation (Eq. 1) are expected to depend on p . In this paper, we will simulate the model with $p = 0.25$ ($p = 0$ is the pure CRSOS model).

The above models were simulated in $d = 1$ in lattices of lengths ranging from $L = 16$ to $L = 1024$ for the CRSOS model with $H_{\max} = 1$ and $H_{\max} = 2$, from $L = 16$ to $L = 256$ for the DT model and from $L = 16$ to $L = 512$ for the competitive model. For the CRSOS models, the number of realizations up to the steady state was typically 10^4 for the smallest lattices and nearly 500 for the largest lattices. The same applies to the DT model, but notice that the largest length in that case was just $L = 256$. In $d = 2$, the CRSOS model with

$H_{\max} = 1$ was simulated in lattices of lengths ranging from $L = 16$ to $L = 256$, and with $H_{\max} = 2$ only until $L = 128$. Whenever the number of realizations up to the steady state was smaller than 10^4 , a larger number of realizations covering the growth and the crossover regions was generated. This allowed the calculation of crossover times (see below) with good accuracy in $d = 1$.

The calculation of the moments of the height distribution at the steady states, W_n (Eq. 6), followed the same lines described in Ref. [13]. In order to estimate dynamical exponents, we used a recently proposed method to calculate a characteristic time τ_0 which is proportional to the time of relaxation to the steady state [30]. For fixed L , after calculating the saturation width $w_{\text{sat}}(L)$, τ_0 is defined through

$$(L; \tau_0) = k_{\text{sat}}(L); \quad (10)$$

with a constant $k < 1$. From the Family-Vicsek relation [31], it is expected that [30]

$$\tau_0 \propto L^z; \quad (11)$$

Here, we estimated τ_0 with k ranging from $k = 0.4$ to $k = 0.7$. Since the exponent z is large, the characteristic times τ_0 increase very fast with L . Consequently, for large k , the accuracy of τ_0 is low in large lattices. On the other hand, for small k , the times τ_0 in small lattices are also very small (near $\tau_0 = 1$) and, consequently, there are effects of the initial state at substrate. This is the reason why we chose a restricted range of k to analyze our data.

III. SCALING EXPONENTS IN ONE-DIMENSIONAL SUBSTRATES

In order to estimate the roughness exponent from the interface width, the first step is to calculate the effective exponents

$$\alpha_{(L;i)} = \frac{\ln [\text{sat}(L) - \text{sat}(L=i)]}{\ln i} \quad (12)$$

for fixed i . It is expected that $\alpha_{(L;i)} \rightarrow H_{\text{max}}$ for any choice of i .

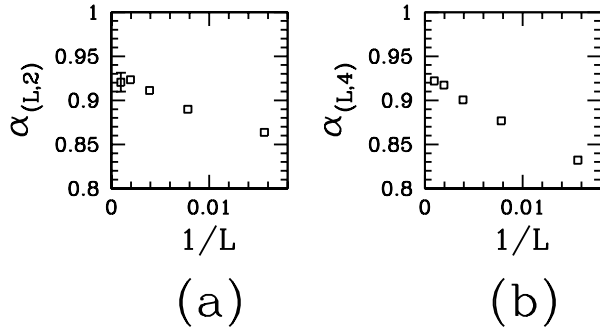


FIG. 1. Effective roughness exponents (a) $\alpha_{(L;2)}$ and (b) $\alpha_{(L;4)}$ versus inverse lattice length for the 1+1-dimensional CRSS model with $H_{\text{max}} = 1$. Error bars are shown only when they are larger than the size of the data points.

In Figs. 1a and 1b we show $\alpha_{(L;2)}$ and $\alpha_{(L;4)}$ versus $1/L$, respectively, for the CRSS model with $H_{\text{max}} = 1$. The evolution of the data suggests that $\alpha_{(L;i)}$ converges to 0.91–0.94, accounting for the error bars and reasonable finite-size corrections.

The type of plot in Figs. 1a and 1b is suitable to fit the data to the scaling form

$$\alpha_{(L;i)} = \frac{2}{i} + AL^{-2}; \quad (13)$$

with A constant, if the correct variable L^{-2} is used in the abscissa ($i = 1$ was tested in Figs. 1a and 1b). In its turn, Eq. (13) is a consequence of a scaling relation $\text{sat} \sim L^{-2}(a_0 + a_1 L^{-2})$, with a_0 and a_1 constants, which includes a sub-dominant term in addition to the dominant one in Eq. (4). However, no variable of the form L^{-2} provided a reasonable linear fit in the range of lattice size analyzed there. Thus, $i = 1$ was used in Figs. 1a and 1b just to illustrate the L -dependence of

the effective exponents. On the other hand, estimating the asymptotic is possible because there is no evidence of an upward curvature of those plots for large L .

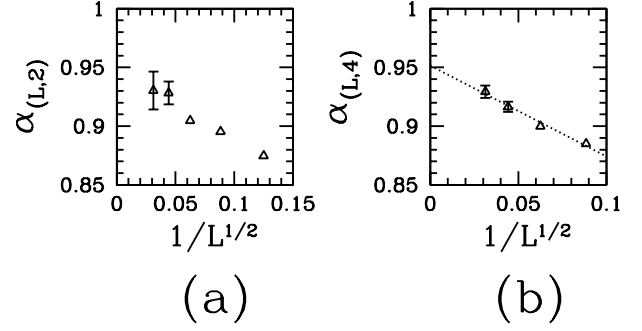


FIG. 2. Effective roughness exponents (a) $\alpha_{(L;2)}$ and (b) $\alpha_{(L;4)}$ versus $1/L^{1/2}$ for the 1+1-dimensional CRSS model with $H_{\text{max}} = 2$. Error bars are shown only when they are larger than the size of the data points.

The data for the CRSS model with $H_{\text{max}} = 2$ was analyzed along the same lines. In Figs. 2a and 2b we show $\alpha_{(L;2)}$ and $\alpha_{(L;4)}$ versus $1/L^{1/2}$, respectively. The variable in the abscissa of Figs. 2a and 2b was chosen to provide a good linear fit of the $\alpha_{(L;4)}$ data – see dotted line in Fig. 2b. These results suggest stronger finite-size corrections for $\alpha_{(L;i)}$ when compared to the model with $H_{\text{max}} = 1$. The corresponding asymptotic estimates are in the range 0.92–0.97, also accounting for the error bars. However, since these error bars are larger than those for $H_{\text{max}} = 1$, it is possible that the true asymptotic regime was not attained yet and that the true leading corrections are different. Anyway, those results still suggest that $\alpha_{(L;i)} < 1$ in the $L \rightarrow \infty$ limit.

Alternatively, we will analyze our data assuming the presence of a constant term as the sub-leading correction to the scaling of sat^2 :

$$\text{sat}^2 = \frac{2}{i} + AL^{-2}; \quad (14)$$

(since $i = 1$, it corresponds asymptotically to $\frac{2}{i} = 2$ in Eq. 13). $\frac{2}{i}$ is called intrinsic width and is frequently associated to large local slopes in discrete KPZ models [25,26,13]. Effective exponents $\alpha_L^{(I)}$ which cancel the contribution of $\frac{2}{i}$ may be defined as

$$\alpha_L^{(I)} = \frac{1}{2} \frac{\ln \frac{W_{4,\text{sat}}(2L)}{W_{4,\text{sat}}(L)}}{\ln 2} = \frac{W_{4,\text{sat}}(L)}{W_{4,\text{sat}}(L=2)}; \quad (15)$$

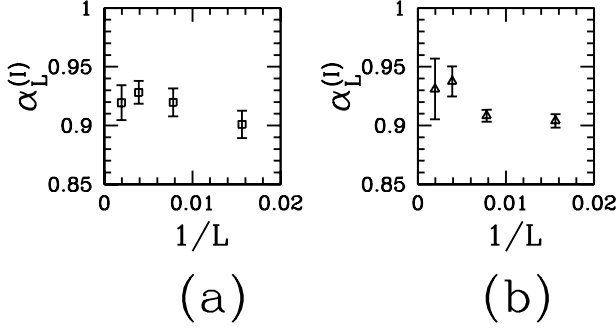


FIG. 3. Effective roughness exponents $\alpha_L^{(I)}$ (accounting for the intrinsic width) versus $1/L$ for 1+1-dimensional CRSOS models with (a) $H_{\text{max}} = 1$ and (b) $H_{\text{max}} = 2$.

In Figs. 3a and 3b we show $\alpha_L^{(I)}$ versus $1/L$ for the CRSOS model with $H_{\text{max}} = 1$ and $H_{\text{max}} = 2$, respectively. Here, the variable $1/L$ in the abscissa was also not chosen to perform data extrapolation. The effective exponents vary within narrow ranges (0.89 to 0.94 for $H_{\text{max}} = 1$, 0.90 to 0.96 for $H_{\text{max}} = 2$), even including their error bars. Consequently, any variable in the form L^{α} (0.5 to 2) leads to nearly the same extrapolated value of α . The data for $H_{\text{max}} = 1$ are more accurate and suggests 0.90 to 0.95, which is consistent with the previous analysis. The results for $H_{\text{max}} = 2$ confirm the trend to $\alpha < 1$, although the uncertainties are larger.

Assuming the power-counting property (Eq. 7) of the moments of the width distribution (to be discussed in detail in Sec. V), we may also use higher moments to estimate α . The effective exponents obtained from W_3 have large fluctuations, but those obtained from W_4 behave similarly to the ones obtained from the interface width. They are defined as

$$\alpha_{(L;2)}^{(4)} = \frac{\ln [W_{4,\text{sat}}(L)/W_{4,\text{sat}}(L=i)]}{\ln i}; \quad (16)$$

where $W_{4,\text{sat}}(L)$ are the fourth moments calculated at the steady states.

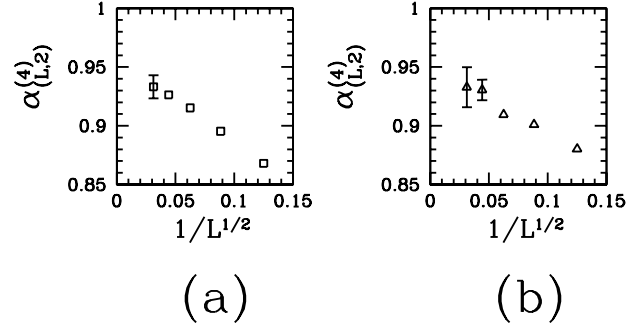


FIG. 4. Effective roughness exponents $\alpha_{(L;2)}^{(4)}$ (obtained from the fourth moment W_4) versus $1/L^{1/2}$ for 1+1-dimensional CRSOS models with (a) $H_{\text{max}} = 1$ and (b) $H_{\text{max}} = 2$. Error bars are shown only when they are larger than the size of the data points.

In Figs. 4a and 4b we show $\alpha_{(L;2)}^{(4)}$ versus $1/L^{1/2}$ for the CRSOS models with $H_{\text{max}} = 1$ and $H_{\text{max}} = 2$, respectively. The variable in the abscissa of Figs. 4a and 4b was also chosen to illustrate the behavior of the data for large L and not to fit the data to a certain scaling form. The downward curvature of the plots for large L also suggest $\alpha < 1$. The maximum and minimum reasonable limits that can be inferred from the evolution of the data for $H_{\text{max}} = 1$ give 0.92 to 0.96. The accuracy of the estimate for $H_{\text{max}} = 2$ is lower, as before.

The intersection of at least two of the above estimates for $H_{\text{max}} = 1$, obtained from the scaling of different quantities and assuming different forms of finite-size corrections, provides a final estimate $\alpha = 0.94 \pm 0.02$. As will be discussed below, results for the DT model do not improve those obtained with the CRSOS model.

In Figs. 5a and 5b we show the effective exponents $\alpha_{(L;2)}^{(4)}$ and $\alpha_{(L;2)}^{(4)}$ for the noise-reduced DT model, also as a function of $1/L^{1/2}$. They are larger than $\alpha = 1$ and systematically increase with L . However, from all previous theoretical work and the above numerical data for the CRSOS models, there is no reason to expect $\alpha > 1$ in the VLD S class. Consequently, extrapolation of those data will not give reliable information for the discussion on the exponents of the VLD S theory in 1+1 dimensions. Instead, it is expected that the effective exponents for the noise-reduced DT model (Figs. 5a and 5b) will eventually begin to decrease with L , possibly for much larger L . Such decrease of $\alpha_{(L;2)}^{(4)}$ is actually observed in the original

DT model (without noise reduction), in the same range of lattice lengths analyzed here [27]. Also recall that, as shown in Ref. [27], the data for original DT model also present huge finite-size effects and cannot be used to obtain reliable estimates of VLD S exponents.

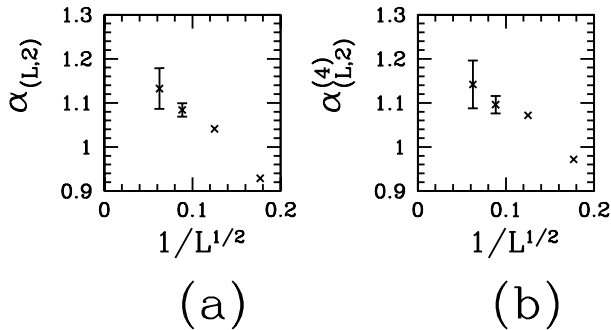


FIG. 5. Effective roughness exponents (a) $\alpha_{(L,2)}$ (obtained from the interface width) and (b) $\alpha_{(L,2)}^{(4)}$ (obtained from W_4) versus $1/L^{1/2}$ for the 1+1-dimensional DT model. Error bars are shown only when they are larger than the size of the data points.

No improvement of the results in Figs. 5a and 5b is obtained by considering the contribution of the intrinsic width (Eqs. 14 and 15).

There are other two points concerning our results for the DT model that deserve some comments. The first one is the comparison with results of Panyindu and Dasgupta in Ref. [24], who obtained $\alpha = 1$ with noise reduction in lattice lengths $L < 60$. Our effective exponents for the smallest lattices ($16 \leq L \leq 64$) correspond to two data points at the left sides (larger $1/L$) of Figs. 5a and 5b and those exponents are also near $\alpha = 1$. Consequently, our estimates are consistent with those of Ref. [24]. On the other hand, we conclude that the noise-reduction scheme works properly only in a special range of lattice lengths, since its application to larger lattices ($L = 128$ and $L = 256$ in Figs. 5a and 5b) led to effective exponents larger than 1, indicating much more complicated finite-size behavior.

The other important point is related to the large error bars, particularly for $L = 256$. One of the reasons is certainly the relatively small number of realizations for the largest lengths (see Sec. II). However, the surfaces generated by the DT model in $d = 1$ present grooves which may survive during long times. These structures

largely increase the interface width of some realizations (see Ref. [32]) and, consequently, have remarkable influence on the fluctuations of that quantity when averaged over various realizations. However, note that this instability is controlled in the DT model, i. e. the depths of the grooves do not diverge as time increases, contrary to other discretized growth models which show true instabilities when pillars or grooves are formed [32,33].

Now we turn to the calculation of the dynamical exponent.

Effective dynamical exponents are defined as

$$z_{(L,i)} = \frac{\ln [\sigma_0(L) = \sigma_0(L=i)]}{\ln i}; \quad (17)$$

so that $z_L \rightarrow z$ as $t \rightarrow 1$. The error bars of σ_0 are larger than those of σ and the uncertainties are enlarged in the calculation of effective exponents for small values of i (Eq. 17), then we will work only with $i = 4$.

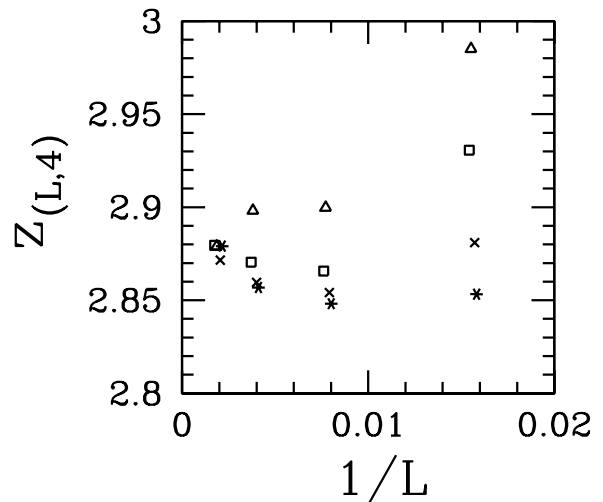


FIG. 6. Effective dynamical exponents $z_{(L,4)}$ versus $1/L$ for the 1+1-dimensional CRSOS model with $H_{\max} = 1$. Small horizontal shifts of the data points were used to avoid their superposition. Error bars (not shown) are smaller than $z = 0.02$ (of this order for the largest L).

In Fig. 6 we show $z_{(L,4)}$ versus $1/L$ for the CRSOS model with $H_{\max} = 1$, with σ_0 calculated using four different values of k in Eq. (10) ($0.4 \leq k \leq 0.7$). The data for different k clearly converge to the same region, providing an asymptotic estimate $z = 2.88 \pm 0.04$. This estimate also accounts for the error bars (not shown in Fig. 6), which are near $z = 0.02$ for the largest values of L . Again it is clear that the value $z = 3$ of one-loop renormalization is excluded.

This conclusion is corroborated by the results for the CRSOS model with $H_{\max} = 2$, although the accuracy

of the data was poorer. In Fig. 7 we show $z_{(L,4)}$ versus $1/L$ for that model, with τ_0 also calculated using four different values of k in Eq. (10).

Our results for the noise-reduced DT model do not provide useful information on dynamic exponents, similarly to the case of the roughness exponents.

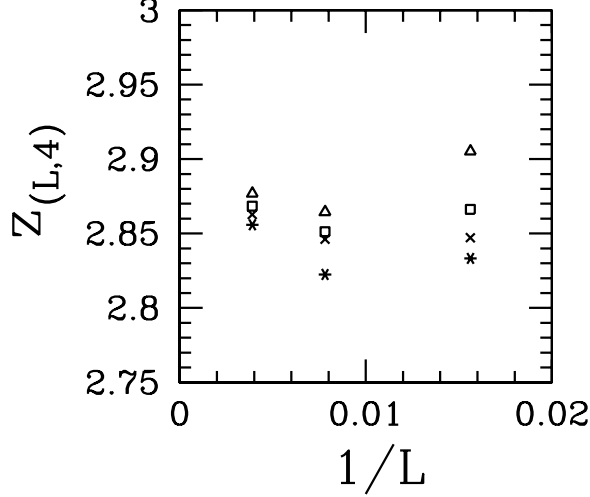


FIG. 7. Effective dynamic exponents $z_{(L,4)}$ versus $1/L$ for the 1+1-dimensional CRSOS model with $H_{\max} = 2$. Error bars (not shown) are smaller than $z = 0.03$ (of this order for the largest L).

IV. SCALING EXPONENTS IN TWO-DIMENSIONAL SUBSTRATES

In Figs. 8a and 8b we show $\alpha_{(L,2)}$ (Eq. 12) and $\alpha_{(L,2)}^{(4)}$ (Eq. 16) for the two-dimensional CRSOS model with $H_{\max} = 1$. Both linear fits give $\alpha = 0.662$, which is very near the one-loop renormalization value $\alpha = 2/3$ of the VLD S theory. Accounting for the error bars, which are particularly large for $L = 256$, we are not able to determine whether $\alpha = 2/3$ is exact or not. On the other hand, comparing other authors' results [10], any difference from that value is probably smaller than the two-loops correction of Janssen [7], which is 0.014 .

Similarly to the one-dimensional case, the error bars of the data for the model with $H_{\max} = 2$ are larger. Consequently, no discrepancy from the one-loop exponents could be detected too.

The characteristic times τ_0 for the model with $H_{\max} = 1$ were obtained in lattices with $16 \leq L \leq 128$, but their values for the smallest lattices ($L = 16$ and $L = 32$) are very small, sometimes below $\tau_0 = 1$ (one monolayer). For $L = 256$, the accuracy of the interface widths data is not enough to provide reliable estimates of

τ_0 . Consequently, we were not able to calculate accurate dynamic exponents in the two-dimensional case.

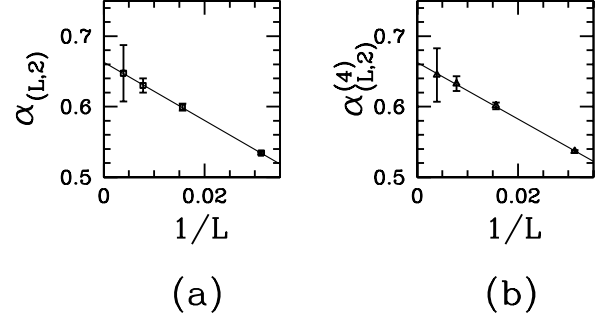


FIG. 8. Effective roughness exponents (a) $\alpha_{(L,2)}$ (obtained from the interface width) and (b) $\alpha_{(L,2)}^{(4)}$ (obtained from W_4) versus $1/L$ for the 2+1-dimensional CRSOS model with $H_{\max} = 1$. Error bars are shown only when they are larger than the size of the data points.

V. UNIVERSALITY OF AMPLITUDE RATIOS

Evidence on the power-counting property of the moments W_n of the heights distribution of VLD S models was given in Sec. III by the estimates of α obtained from W_2 and W_4 . A clearer evidence is given here by the finite asymptotic estimates of the skewness and the kurtosis at the steady states.

First we consider the models in 1+1 dimensions.

In Figs. 9a and 9b we show the steady state skewness versus $1/L^{1/2}$ for the CRSOS models with $H_{\max} = 1$ and $H_{\max} = 2$, respectively. Except for the data for $L = 1024$, which have relatively large error bars, all points fall in almost perfect straight lines, which give the asymptotic value $S = 0.32 \pm 0.02$ for both models.

In Figs. 9c and 9d we show the steady state kurtosis versus $1/L^{1/2}$ for the CRSOS models with $H_{\max} = 1$ and $H_{\max} = 2$, respectively. Only the data for $L = 512$ were shown because the error bars are much larger for $L = 1024$, not giving additional information on the evolution of Q . Reasonable linear fits are obtained with the last four data points in each case. The asymptotic estimate is $Q = 0.11 \pm 0.02$ for both models.

Our results for the competitive model (RD and CRSOS) introduced in Sec. II also suggest that those amplitude ratios are universal for VLD S models. In that case,

there is no constraint on the difference of the heights of neighboring columns, but only a trend to suppress large heights differences. The coefficients β_4 and β_4 in the corresponding continuous equation (Eq. 1) are probably different from those in the pure model ($p = 0$), as obtained in related competitive models [28,29]. In Figs. 10a and 10b we show, respectively, $S(L; t \rightarrow \infty)$ and $Q(L; t \rightarrow \infty)$ as a function of $1/L^{1/2}$ for the competitive model. The asymptotic estimates are $S = 0.32 \pm 0.02$ and $Q = 0.1$, which are near the previous estimates for the pure CRSS model.

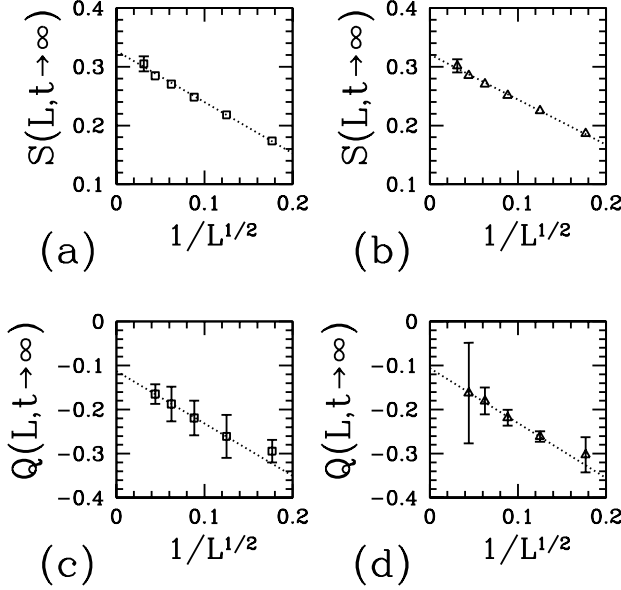


FIG. 9. Steady state skewness for the 1 + 1-dimensional CRSS model with (a) $H_{\max} = 1$ and (b) $H_{\max} = 2$, and steady state kurtosis for that model with (c) $H_{\max} = 1$ and (d) $H_{\max} = 2$, as functions of $1/L^{1/2}$. Dotted lines are least squares fits of the data. Error bars are shown only when they are larger than the size of the data points.

In Figs. 10c and 10d we show, respectively, $S(L; t \rightarrow \infty)$ and $Q(L; t \rightarrow \infty)$ as a function of $1/L^{1/2}$ for the noise-reduced DT model in $d = 1$. There are several reasons for the large error bars of the kurtosis, particularly in the largest lattices. Firstly, as justified in Sec. III, fluctuations in the data for the DT model are typically large. Secondly, the relative fluctuations of the moments W_n (Eq. 6) rapidly increase with the order n . Finally, while the size of the error bar of the kurtosis is the same of $W_4 = W_2^2$, the relative error significantly increases when the constant 3 is subtracted (Eq. 9). The relatively large errors in Figs. 9c and 9d (CRSS models) can also be explained along these lines.

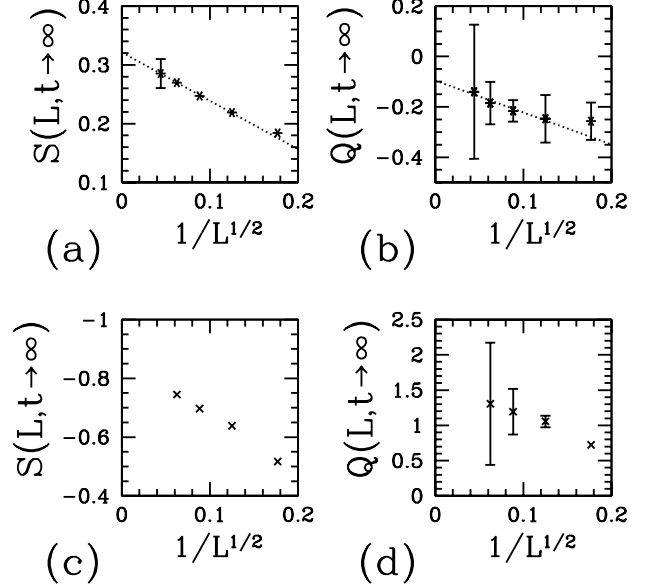


FIG. 10. (a), (b): steady state skewness and kurtosis, respectively, as a function of $1/L^{1/2}$, for the competitive model (CRSS with $H_{\max} = 1$ and RD); (c), (d): steady state skewness and kurtosis, respectively, as a function of $1/L^{1/2}$, for the DT model. Dotted lines are least squares fits of the data. Error bars are shown only when they are larger than the size of the data points.

The trends of the data for the DT model in Figs. 10c and 10d are completely different from those of the CRSS models. We cannot exclude the possibility that the universality of the amplitude ratios be a special feature of CRSS models and some simple extensions, like the above competitive model. However, the behavior of the scaling exponents of the DT model is also unusual, with no possible extrapolation to the expected region of the VLD theory ($\beta_1, z = 3$), as discussed in Sec. III. Consequently, the present results for the DT model, although not confirming the universality of the amplitude ratios, are not reliable to discard that hypothesis (the negative sign of the skewness is not a problem, since its sign changes with β_4 —see related discussion in Ref. [13]).

Now we turn to the CRSS models in 2 + 1 dimensions.

In Figs. 11a and 11b we show the steady state skewness versus $1/L^{1/2}$ for the CRSS models with $H_{\max} = 1$ and $H_{\max} = 2$, respectively. The asymptotic estimates are $S = 0.19 \pm 0.02$ and $S = 0.20 \pm 0.02$, which also suggest the universality of this quantity. In Figs. 11c and 11d we show the steady state kurtosis versus $1/L^{1/2}$ for the CRSS models with $H_{\max} = 1$ and $H_{\max} = 2$, respectively. The asymptotic value $Q = 0$, which is the Gaussian value, is consistent with the error bars. Thus, in 2 + 1 dimensions, we also obtain evidence of universality of the amplitude ratios for CRSS models, which suggests this possibility for the whole VLD class.

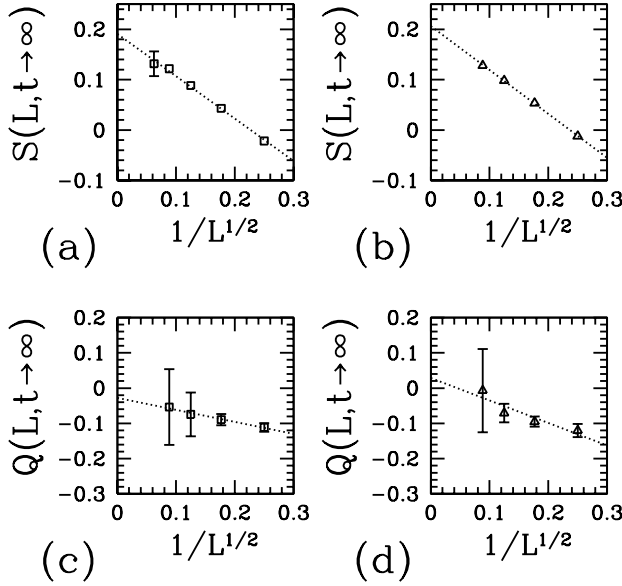


FIG. 11. Steady state skewness for the $2 + 1$ -dimensional CRSS model with (a) $H_{\max} = 1$ and (b) $H_{\max} = 2$, and steady state kurtosis for that model with (c) $H_{\max} = 1$ and (d) $H_{\max} = 2$, as functions of $1/L^{1/2}$. Dotted lines are least squares fits of the data. Error bars are shown only when they are larger than the size of the data points.

VI. SUMMARY AND CONCLUSION

We studied numerically discrete growth models which belong to the VLD S class in $1 + 1$ and $2 + 1$ dimensions. Scaling exponents and steady state values of the skewness and the kurtosis, which characterize the heights distribution, were determined for those models.

Results for the CRSS model with $H_{\max} = 1$ gave the roughness exponent $\chi = 0.94 \pm 0.02$ and the dynamical exponent $z = 2.88 \pm 0.04$ in $d = 1$. These estimates confirm the proposal of Janssen [7] that the exponents of the VLD S theory obtained from one-loop renormalization ($\chi = 1$ and $z = 3$) are not exact. The corrections from two-loops calculations give $\chi = 0.97$ and $z = 2.94$, but they are obtained from expansions in $4 - d$, which are not expected to provide accurate results for small d . On the other hand, the negative sign of the correction to one-loop results is consistent with our findings. In $d = 2$, our results are not able to exclude the one-loop values, confirming other authors' conclusions [10].

The estimates of the steady state skewness and kurtosis of the CRSS models with $H_{\max} = 1$ and $H_{\max} = 2$ and of the competitive model (RD versus CRSS with

$H_{\max} = 1$) suggest that those amplitude ratios are universal in the VLD S class. However, for the DT model in $d = 1$, which belongs to the same class, those quantities are very different from the suggested universal values. One possible reason for this discrepancy is the slow con-

vergence of the DT data to the VLD S behavior. The hypothesis of a slow crossover is supported by the fact that the estimates of χ for the DT model are significantly larger than the values predicted theoretically and confirmed numerically ($\chi = 1$ in $d = 1$). Another possibility is that both CRSS models and the competitive model have continuum representations with suitable combinations of coefficients which lead to the same forms of the heights distributions.

We believe that the results of this work will motivate further studies, numerical and analytical, of the VLD S equation and related discrete models. The estimates of scaling exponents in $d = 1$ and the apparent universality of amplitude ratios are some of the results that may eventually help one to validate approximations in analytical works. On the other hand, numerical solutions of the VLD S equation or simulations of new discrete models in this class would be relevant to broaden the present discussion.

Acknowledgements

The author thanks useful suggestions of Prof. H. K. Janssen and Prof. S. Das Samra.

This work was partially supported by CNPq and FAPERJ (Brazilian agencies).

-
- [1] A.-L. Barabasi and H. E. Stanley, *Fractal Concepts in Surface Growth* (Cambridge University Press, New York, 1995).
 - [2] J. Krug, *Adv. Phys.* **46**, 139 (1997).
 - [3] J. Villain, *J. Phys. I* **1** (1991) 19.
 - [4] Z.-W. Lai and S. Das Samra, *Phys. Rev. Lett.* **66** (1991) 2348.
 - [5] M. Kardar, G. Parisi and Y.-C. Zhang, *Phys. Rev. Lett.* **56** (1986) 889.
 - [6] E. Katzav, *Phys. Rev. E* **65**, 32103 (2002).
 - [7] H. K. Janssen, *Phys. Rev. Lett.* **78**, 1082 (1997).
 - [8] Y. Kim, D. K. Park and J. M. Kim, *J. Phys. A: Math. Gen.* **27**, L533 (1994).
 - [9] Y. Kim and J.-M. Kim, *Phys. Rev. E* **55**, 3977 (1997).
 - [10] S. H. Yook, J. M. Kim and Y. Kim, *Phys. Rev. E* **56**, 4085 (1997).
 - [11] C.-S. Chin and M. den Nijs, *Phys. Rev. E* **59**, 2633 (1999).
 - [12] E. Marinari, A. Pagnani and G. Parisi, *J. Phys. A* **33**, 8181 (2000).
 - [13] F. D. A. Azaõ Reis, *Phys. Rev. E* **69**, 21610 (2004).
 - [14] S. Das Samra and P. Tamborenea, *Phys. Rev. Lett.* **66** (1991) 325.
 - [15] S. Das Samra, P. P. Chatrathom, and Z. Toroczka, *Phys. Rev. E* **65** (2002) 036144.
 - [16] A. Chame and F. D. A. Azaõ Reis, *Surf. Sci.* **553**, 145

- (2004).
- [17] Z.-F. Huang and B.-L. Gu, Phys. Rev. E 57, 4480 (1998).
 - [18] S.-C. Park, D. Kim and J.-M. Park, Phys. Rev. E 65, 15102 (2002).
 - [19] S.-C. Park, J.-M. Park, and D. Kim, Phys. Rev. E 65, 36108 (2002).
 - [20] J.M. Kim and J.M. Osterlitz, Phys. Rev. Lett. 62 2289 (1989).
 - [21] J.M. Kim, J.M. Osterlitz and T. Ala-Nissila, J. Phys. A : Math. Gen. 24, 5569 (1991).
 - [22] F.D.A. Araujo Reis and D.F. Franceschini, Phys. Rev. E 61, 3417 (2000).
 - [23] W.E. Hagston and H. Ketterl, Phys. Rev. E 59, 2699 (1999).
 - [24] P. Punyindu and S. Das Sarm a, Phys. Rev. E 57 (1998) R 4863.
 - [25] D.E. Wolf and J. Kertesz, Europhys. Lett. 4, 651 (1987).
 - [26] J. Kertesz and D.E. Wolf, J. Phys. A 21, 747 (1988).
 - [27] B.S. Costa, J.A.R. Euzébio, and F.D.A. Araujo Reis, Physica A 328, 193 (2003).
 - [28] C.M. Horowitz and E. Albano, J. Phys. A : Math. Gen. 34 357 (2001).
 - [29] C.M. Horowitz, R.A. Monetti, E.V. Albano, Phys. Rev. E 63 66132 (2001).
 - [30] F.D.A. Araujo Reis, Physica A 316 250 (2002).
 - [31] F. Family and T. Vicsek, J. Phys. A 18 L75 (1985).
 - [32] C. Dasgupta, J.M. Kim, M. Dutta, and S. Das Sarm a, Phys. Rev. E 55, 2235 (1997).
 - [33] C. Dasgupta, S. Das Sarm a, and J.M. Kim, Phys. Rev. E 54, R 4552 (1996).